

State Transitions and Decoherence in the Avian Compass

Vishvendra Singh Poonia,* Dipankar Saha, and Swaroop Ganguly†

*Department of Electrical Engineering,
Indian Institute of Technology Bombay,
Mumbai – 400076, India*

(Dated: June 16, 2021)

The radical pair model has been successful in explaining behavioral characteristics of the geomagnetic compass believed to underlie the navigation capability of certain avian species. In this study, the spin dynamics of the radical pair model and decoherence therein are interpreted from a microscopic state transition point of view. This helps to elucidate the interplay between the hyperfine and Zeeman interactions that enables the avian compass, and the distinctive effects of nuclear and environmental decoherence on it. Using a quantum information theoretic quantifier of coherence, we find that nuclear decoherence induces new structure in the spin dynamics without materially affecting the compass action; environmental decoherence, on the other hand, completely disrupts it.

PACS numbers: Valid PACS appear here

I. INTRODUCTION

Overt quantum effects seem to play a key role in the functionality of a number of biological systems, e.g. excitonic transport in photosynthetic pigments, coherent spin dynamics in avian magnetoreception, inelastic electron tunneling in olfaction, and hydrogen tunneling in enzyme catalysis [1–11]. This is not only intriguing from a physics perspective – given the noisy high-temperature ambience in these situations – but also promises to reveal robust ways to harness ‘quantumness’ for engineering new and improved systems, both biomimetic and otherwise.

In this work we study avian magnetoreception, which is responsible for the geomagnetic field assisted navigation ability of various bird species [9, 10]. A radical pair (RP) model, comprising photo-excited unpaired spins along with an anisotropic hyperfine interaction, has been proposed as a possible mechanism [12–15]. This kind of a model is supported both by spin chemistry findings [16–19] and by behavioral experiments on certain bird species, e.g. the European Robin [11, 13, 20, 21].

One of the central quests in RP model studies is the determination of the role of quantum effects especially coherence, including nuclear and environmental decoherence effects, in the spin dynamics [22–26]. A few groups [21, 23, 27, 28] have established the presence of long coherence in RP spin states. Others [25] have quantified coherence using a quantum interferometer analogy and statistically concluded that global electron-nuclear coherence is a resource for chemical compass by observing sensitivity as a function of global coherence. Tiersch and Briegel identify nuclear decoherence as a necessary ingredient for the magnetosensitive spin dynamics of the RP system [22]. Apart from coherence, Gauger et al. and Cai et al. have studied the role of entanglement

in the compass action of the RP model [24, 27]. However, the distinct operational role of nuclear and environmental decoherence in RP spin dynamics is still unclear. Understanding this is essential to the appropriate selection/engineering of materials for solid state emulation of RP spin dynamics, and possibly other quantum biomimetic applications.

In this work, we take a microscopic view of radical pair spin dynamics, analyzing the distinctive role of nuclear and environmental decoherence, and examine their specific effects in its magnetosensitive behavior. We look at the state transitions involved in radical pair spin state evolution and elucidate the effect of nuclear and environmental decoherence on these transitions. Our conclusions are validated by applying an information theoretic measure of coherence. Further, our spin transition point of view provides new insights into the role of Zeeman and hyperfine interactions in the magnetosensitive dynamics of the RP spin system. We also revisit some of earlier RP model results from this new perspective.

The salient characteristics of avian magnetoreception have been demonstrated by multiple behavioral experiments. Firstly, it exhibits a certain dynamic range around the geomagnetic field. This dynamic range behavior is versatile, in that it adapts to a new Zeeman field if the bird is exposed long enough to it [21]. Secondly, the compass action is found to be disrupted by an external RF field of a particular frequency. Both of these features are, in fact, well-explained within the RP model [21, 23, 29].

In the RP system, we effectively have a three spin system evolving under a Hamiltonian that contains two interactions – hyperfine and Zeeman. The singlet and triplet radicals recombine distinctly thus leading to different products. The final yield corresponding to singlet and triplet states depends on the magnetic field. Strikingly, however, we find that the Zeeman interaction alone is not sufficient to make the final yields dependent on the magnetic field orientation (angle between geomagnetic field

* vishvendra@iitb.ac.in

† sganguly@ee.iitb.ac.in

and radical pair axis); neither can the hyperfine interaction on its own cause spin transitions from the singlet to all three triplet states, and thereby impart magnetic sensitivity. It is the interplay between the Zeeman and the hyperfine interactions that makes the overall spin dynamics magnetosensitive.

This paper is organized as follows: In Sec. II, we investigate the state transitions involved in the RP spin dynamics. In Sec. III and IV, we examine the roles of nuclear and environmental decoherence respectively. In Sec. V, we present our conclusions and perspective for solid state emulation of the avian compass.

II. SPIN DYNAMICS OF THE RADICAL PAIR

In order to study the spin transitions involved in the RP dynamics, we choose a representative RP system in which an unpaired spin on each of two radicals, and a single nucleus on one of them is responsible for an hyperfine interaction therein. This model may be directly extrapolated to multinuclear systems [27, 30]. The nucleus preferentially interacts with the spin on the same radical and both the spins interact with the geomagnetic Zeeman field. Therefore, the RP Hamiltonian looks like [27]:

$$H = \gamma \mathbf{B} \cdot (\hat{S}_1 + \hat{S}_2) + \hat{I} \cdot \mathbf{A} \cdot \hat{S}_2 \quad (1)$$

\hat{S}_1 and \hat{S}_2 are electron spin operators, and \hat{I} is the nuclear spin operator given as: $\hat{I}, \hat{S}_1, \hat{S}_2 \in \frac{1}{2}(\sigma_x, \sigma_y, \sigma_z)$, $\gamma = \mu_0 g$ is gyromagnetic ratio, μ_0 is Bohr magneton and g is electron g-factor ($= 2$). We consider the illustrative case in which the hyperfine tensor $\mathbf{A} = \text{diag}(0, 0, a)$ [30]. The external field (geomagnetic field) is characterized by $\mathbf{B} = B_0(\sin\theta\cos\phi, \sin\theta\sin\phi, \cos\theta)$; $B_0 (= 47\mu T)$ is the local geomagnetic field at Frankfurt [21] and θ is the magnetic field orientation. The axial symmetry of hyperfine tensor allows us to take $\phi = 0$ [27]. The RP spin dynamics starts at the instant of radical pair generation, which is taken to be $t = 0$. The initial state of the radical pair is usually taken to be singlet state ($|s\rangle$) with the nuclear spin completely depolarized owing to its interaction with the neighboring soft matter environment [13, 27, 31]. We adopt the quantum master equation approach to simulate the dynamics of the RP system, similar to Gauger et al. [27] but modified to highlight the exact spin transitions. Intrinsically, the Hilbert space is eight dimensional. The spin-dependent relaxation process happens through two channels – the singlet channel whereby radical pairs in the $|s\rangle$ state recombine and triplet channel whereby radical pairs in the three triplet states $|t_0\rangle$, $|t_-\rangle$ and $|t_+\rangle$ recombine – which are included as ‘shelving’ states in the Hilbert space. In order to distinguish the spin transitions, we resolve the triplet channel into its three constituent channels corresponding to $|t_0\rangle$, $|t_+\rangle$ and $|t_-\rangle$. This is accommodated by augmenting the eight dimensional Hilbert space with four additional shelving states denoted as $|S\rangle$, $|T_0\rangle$, $|T_+\rangle$, and $|T_-\rangle$.

This method is quite versatile for the calculation of the yield corresponding to various spin states. The recombination of radical pair into singlet and triplet channels is modeled through decay operators in the master equation (ME) as: $P_1 = |S\rangle\langle s, \uparrow|$, $P_2 = |S\rangle\langle s, \downarrow|$, $P_3 = |T_0\rangle\langle t_0, \uparrow|$, $P_4 = |T_0\rangle\langle t_0, \downarrow|$, $P_5 = |T_+\rangle\langle t_+, \uparrow|$, $P_6 = |T_+\rangle\langle t_+, \downarrow|$, $P_7 = |T_-\rangle\langle t_-, \uparrow|$ and $P_8 = |T_-\rangle\langle t_-, \downarrow|$. The Lindblad master equation describing the evolution of RP spin system is given by [27]:

$$\dot{\rho} = -\frac{i}{\hbar}[H, \rho] + k \sum_{i=1}^8 P_i \rho P_i^\dagger - \frac{1}{2}(P_i^\dagger P_i \rho + \rho P_i^\dagger P_i) \quad (2)$$

Here k ($= 5 \times 10^5 \text{ s}^{-1}$) is the singlet and triplet radical recombination rate. We note that this method is equivalent to the Haberkorn approach to modeling radical pair dynamics [19, 25, 27] but is more amenable for discerning the spin transitions involved in the compass action. The system starts in the state $\rho(0) = \frac{1}{2}I \otimes (|s\rangle\langle s|)$. The ensuing spin evolution involves intersystem crossing between singlet and triplet states. It is accompanied by a spin dependent recombination process in which singlet and triplet radical pairs recombine through different channels; it is this Zeeman field dependent differen-

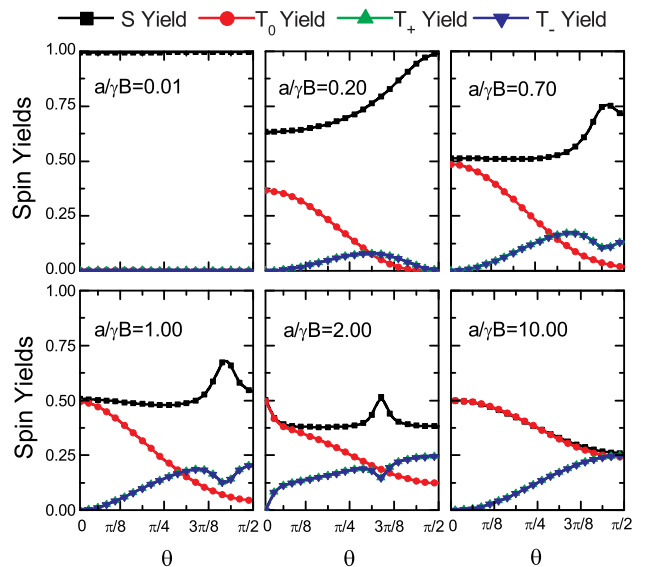


FIG. 1. (Color online) Singlet (S) and triplet (T_0 , T_+ , T_-) yields vs. geomagnetic field orientation for various hyperfine coupling strengths. These figures illustrates how various spin transition pathways between $|s\rangle$, $|t_0\rangle$, $|t_+\rangle$, $|t_-\rangle$ make the final spin yields angle dependent. Simultaneous Zeeman and anisotropic hyperfine plays collaborative role in inducing these transitions which ultimately lead to magnetosensitive product yield. (The various transitions induced by anisotropic hyperfine and Zeeman interactions are shown in the state transition diagram, Fig. 2.) Additionally, we observe a conspicuous peak appearing in S yield for a range of hyperfine constants. This peak corresponds to the dip in T_+ and T_- yields. We recognize that this peak appears due to nuclear decoherence.

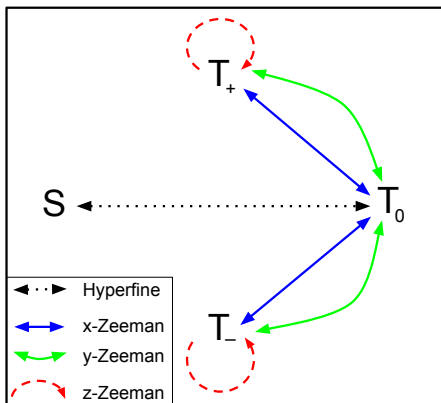


FIG. 2. (Color online) Spin-state transitions for various Hamiltonian interactions.

tial spin yield which is used by the avian neural system to sense the geomagnetic field [12, 27, 30], although the neurological processes involved are not yet fully understood [28]. Our aim in this manuscript is to explain: one, the details of the spin transitions responsible for the magnetosensitive yield, and two, the role of coherent evolution of electron pair spins and decoherence due to nucleus and environment in the overall functioning of chemical compass model of the avian magnetoreception.

In order to examine the spin transitions in the RP model, we simulate RP dynamics for a large number of hyperfine interaction strengths. For our choice of hyperfine coupling tensor, the Hamiltonian looks like: $\hat{H} = \gamma \mathbf{B} \cdot (\hat{S}_1 + \hat{S}_2) + a \hat{I}_z \hat{S}_z$. Here, we vary the hyperfine coupling strength from $\gamma B_0/100$ (very small compared to the Zeeman strength) to $100\gamma B_0$ (very large compared to the Zeeman strength) and examine the singlet and various triplet yields with respect to the orientation of the geomagnetic field. The results are presented in Fig. 1 from which we infer the following spin transitions are associated with various terms in the Hamiltonian:

- (i) The hyperfine interaction induces the $|s\rangle \leftrightarrow |t_0\rangle$ transition but does nothing to $|t_+\rangle$ and $|t_-\rangle$ states.
- (ii) The x-component of Zeeman interaction induces the $|t_-\rangle \leftrightarrow |t_0\rangle \leftrightarrow |t_+\rangle$ transitions but leaves the $|s\rangle$ state alone. Similar is the case with y-component of Zeeman interaction.
- (iii) The z-component of Zeeman interaction does not induce any inter-spin transition.

These results have been confirmed analytically in Appendix A. They are also in agreement with the findings of B. M. Xu et al. where these transitions follow from inspection of the Hamiltonian in $\{|s\rangle, |t_0\rangle, |t_+\rangle, |t_-\rangle\}$ basis [32]. The spin-state transitions induced by the hyperfine and Zeeman interactions as obtained above are summarized in Fig. 2.

For example in Fig. 1, at $\theta = 0^\circ$, the Hamiltonian comprises the hyperfine and z-component of the Zeeman interaction; therefore, in accordance with (i) and (iii), the spin evolution corresponds to the coherent mixing be-

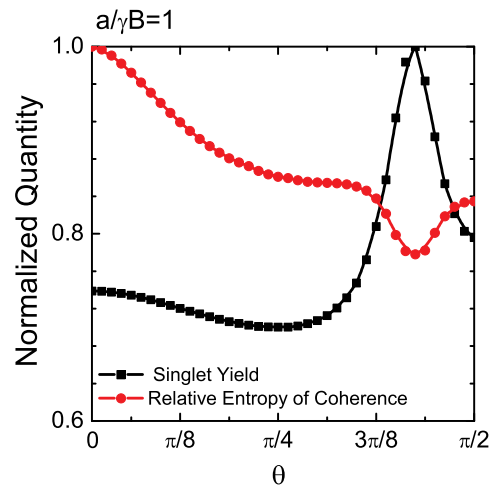


FIG. 3. (Color online) The normalized singlet yield (black) and the normalized relative entropy of coherence (red) as a function of magnetic field orientation θ at $a/\gamma B_0 = 1$. The *relative entropy of coherence* serves as a measure of coherence [33]. The dip in coherence corresponding to the peak in singlet yield indicates that the peaks in singlet yield in Fig. 1 are due to nuclear decoherence. This fact is further affirmed by the singlet yield curve obtained when the nuclear and the radical pair spin states are disentangled, cf. Appendix B.

tween $|s\rangle \leftrightarrow |t_0\rangle$ and the singlet yield saturates at 0.50 for larger hyperfine interaction which corresponds to strong mixing within the recombination timescale. On the other extreme, at $\theta = 90^\circ$, the Hamiltonian comprises the hyperfine interaction and x-component of the Zeeman interaction; based on (i) and (ii), spin transition pathways now exist between all the four spin states by the collective effect of the two interactions and the yields corresponding to all spin states saturate to 0.25 for larger hyperfine interaction strength. Thus, the compass action in the RP model is a consequence of the collective spin dynamical behavior due to the hyperfine and Zeeman interactions.

III. NUCLEAR DECOHERENCE

From Fig. 1, we also observe that there is a conspicuous peak appearing in the singlet yield whose position depends on the hyperfine coupling strength; there are corresponding dips in $|T_+\rangle$ and $|T_-\rangle$ yields suggesting a mechanism that blocks the spin transition pathways from $|s\rangle$ to $|t_+\rangle$ and $|t_-\rangle$. We find that the singlet yield peak vanishes when we disentangle the nuclear and electronic spin dynamics while retaining the effect of the hyperfine interaction, indicating that the peak is actually due to nuclear decoherence. Using a quantum information theoretic quantifier of coherence – the relative entropy of coherence [33] – we seek to establish a connection between the singlet yield peak and nuclear decoherence. The coherence is characterized in the computational basis of the three spin system. If ρ is the density matrix

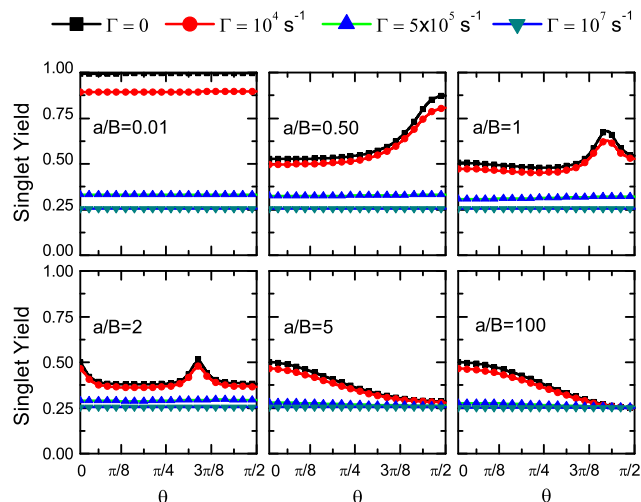


FIG. 4. (Color online) Singlet yield as a function of geomagnetic orientation in presence of environmental noise for the noise rates of $\Gamma = 0 \text{ s}^{-1}$, 10^4 s^{-1} , $5 \times 10^5 \text{ s}^{-1}$, 10^7 s^{-1} . The figure shows that if noise rate is equal to or greater than k , the orientation dependence of the singlet yield is destroyed.

of the system, the relative entropy of coherence is given by [33]:

$$C(\rho) \equiv S(\rho_{diag}) - S(\rho) \quad (3)$$

where $S(\rho)$ is von Neumann entropy corresponding to ρ and ρ_{diag} is obtained by taking only diagonal elements of ρ . The normalized singlet yield and normalized relative entropy of coherence are plotted as a function of magnetic field orientation in Fig. 3. We see a dip in the relative entropy of coherence corresponding to the peak in singlet yield which corroborates our hypothesis that the peak in singlet yield is due to nuclear decoherence.

Defining the sensitivity as: $D_S = \Phi_S^{max} - \Phi_S^{min}$, where Φ_S is the singlet yield and the max/min are with respect to the magnetic field orientation, the aforementioned analysis of singlet yield for various hyperfine interaction strengths reproduces the sensitivity behavior shown by J. Cai et al. [30]. The ripples in their sensitivity vs. $a/\gamma B$ plot (Fig. 1 in that paper) around $a/\gamma B = 1$ can now be understood as a consequence of peaks in the singlet yield and thus a direct manifestation of the nuclear decoherence. Other results reported in that work can also be interpreted along similar lines – that is, by considering the spin state transitions induced by each of the Hamiltonian terms.

IV. ENVIRONMENTAL DECOHERENCE

We adopt the environmental noise model from Gauger et al. [27]. Mathematically, we consider the following six noise operators: $L_1 = I_2 \otimes \sigma_x \otimes I_2$, $L_2 = I_2 \otimes \sigma_y \otimes I_2$, $L_3 = I_2 \otimes \sigma_z \otimes I_2$, $L_4 = I_2 \otimes I_2 \otimes \sigma_x$, $L_5 = I_2 \otimes I_2 \otimes \sigma_y$,

$L_6 = I_2 \otimes I_2 \otimes \sigma_z$. The master equation now gets modified as: $\dot{\rho} = -\frac{i}{\hbar}[H, \rho] + k \sum_{i=1}^8 P_i \rho P_i^\dagger - \frac{1}{2}(P_i^\dagger P_i \rho + \rho P_i^\dagger P_i) + \Gamma \sum_{i=1}^6 L_i \rho L_i^\dagger - \frac{1}{2}(L_i^\dagger L_i \rho + \rho L_i^\dagger L_i)$, where Γ is the noise rate [27]. Fig. 4 shows the singlet yield for four different noise rates, calculated for six different hyperfine coupling strengths. Expectedly, the effect of the environmental noise is most substantial when the noise rate is equal to or greater than the recombination rate k ; in these cases, we find that the compass sensitivity goes to zero. This indicates that environmental noise opens the spin transition pathways between the singlet state and all triplet states and thereby homogenizing the yields corresponding to all the spin states. Therefore, the singlet yield saturates to 0.25, as shown for the case in which the noise rate (Γ) is greater than k .

V. CONCLUSION

In this study, we elucidate the essential spin dynamics of the radical pair model for avian magnetoreception and inspect the distinct effects of nuclear and environmental decoherence therein. We find that the Zeeman and hyperfine interactions play collaborative roles to enable the compass action. In particular, we have identified the dual role played by the nucleus: while the anisotropic nuclear interaction is necessary to induce spin transitions that make the RP dynamics magneto-sensitive, decoherence due to the nucleus introduces additional structure in the dynamics but does not affect the compass action. On the other hand, decoherence due to the environment tends to make the singlet yield insensitive to the geomagnetic field orientation by opening transition pathways between all the spin states; as expected, this destroys the compass action. We think that our approach of understanding the sensitivity of the avian compass – in terms of spin-state transitions induced by each of the Hamiltonian terms, and its limitation – in terms of nuclear and environmental decoherence, may suggest guidelines for its solid state emulation. The diamond nitrogen vacancy center spin system seems to be a potential solid state candidate for this purpose owing to its room temperature long coherence time and two spin relaxation pathways [34–36]. However, a lot of work remains to be done before this, or any other solid state system, can emulate the avian compass and thereby open the path towards geomagnetic field assisted navigation systems.

ACKNOWLEDGMENTS

We are highly grateful to E. M. Gauger, J. Cai, and M. B. Plenio for insightful communications.

Hyperfine Interactions			Zeeman Interactions		
x-hyperfine	y-hyperfine	z-hyperfine	x-Zeeman	y-Zeeman	z-Zeeman
$S \leftrightarrow T_+, T_-$	$S \leftrightarrow T_+, T_-$	$S \leftrightarrow S, T_0$	$S \leftrightarrow S$	$S \leftrightarrow S$	$S \leftrightarrow S$
$T_0 \leftrightarrow T_+, T_-$	$T_0 \leftrightarrow T_+, T_-$	$T_0 \leftrightarrow S, T_0$	$T_0 \leftrightarrow T_+, T_-$	$T_0 \leftrightarrow T_+, T_-$	$T_0 \leftrightarrow T_0$
$T_+ \leftrightarrow T_0, S$	$T_+ \leftrightarrow T_0, S$	$T_+ \leftrightarrow T_+$	$T_+ \leftrightarrow T_0$	$T_+ \leftrightarrow T_0$	$T_+ \leftrightarrow T_+$
$T_- \leftrightarrow T_0, S$	$T_- \leftrightarrow T_0, S$	$T_- \leftrightarrow T_-$	$T_- \leftrightarrow T_0$	$T_- \leftrightarrow T_0$	$T_- \leftrightarrow T_-$

TABLE I: Spin transitions induced by hyperfine and Zeeman interactions.

Appendix A: Spin Transitions due to Hyperfine and Zeeman Interactions

The radical pair Hamiltonian is given in Eq. 1. Under this Hamiltonian, the spin evolution of joint system (radical pair + nucleus) is given by Eq. 2. Here, $\rho = \rho_{nuc} \otimes \rho_{RP}$ is the state of the joint system. At $t=0$, the state of the joint system is given as: $\rho(0) = \frac{1}{2}I \otimes (|s\rangle \langle s|)$.

In order to understand the spin transitions induced by each Hamiltonian interaction, we calculate the density matrix evolution under these Hamiltonian terms. If the Hamiltonian is time independent (which is the case here), the evolution of the density matrix is given as:

$$\rho(t) = e^{-\frac{iHt}{\hbar}} \rho(0) e^{\frac{iHt}{\hbar}} \quad (\text{A1})$$

Under hyperfine part of the Hamiltonian, $H_{hyp} = \hat{I} \cdot \mathbf{A} \cdot \hat{S}_2$, the state of the system evolves as:

$$\rho(t) = e^{-\frac{iH_{hyp}t}{\hbar}} \rho(0) e^{\frac{iH_{hyp}t}{\hbar}} \quad (\text{A2})$$

By tracing out the nuclear part, we get the radical pair state of the Hamiltonian i.e., $\rho_{RP}(t) = \text{tr}_{nuc}(\rho(t))$. Similarly, we can calculate how the radical pair state changes under Zeeman Hamiltonian, $H_{Zeeman} = \gamma \mathbf{B} \cdot (\hat{S}_1 + \hat{S}_2)$. The results of these calculations are summarized in Table. I. These results are also in agreement with the results of B. M. Xu et al. [32].

Appendix B: Nuclear Decoherence

The singlet yield shown in Fig. 1 shows a peak in the curve. The peaks are hypothesized to be due to nuclear decoherence which is also verified by quantifying the nuclear decoherence by relative entropy [33], shown in Fig. 3. Here, we present yet another evidence that the singlet yield peaks are the consequence of nuclear decoherence. We calculate the singlet yield by disentangling the radical pair state from the nuclear state i.e. instead of taking hyperfine interaction as $H_{hf} = \hat{I} \cdot \mathbf{A} \cdot \hat{S}_2 =$

$\sum_{i=x,y,z} \sigma_i \otimes I \otimes \sigma_i$, we consider the *modified hyperfine interaction*: $H_{mhf} = \sum_{i=x,y,z} I \otimes I \otimes \sigma_i$; this eliminates the

evolution of the nuclear state and effectively treats the nuclear spin as a source of static magnetic field acting on one of the RP spins. Fig. 5 shows the singlet yield for a number of modified hyperfine interaction strengths. Comparing with Fig. 1, we can clearly see that now the

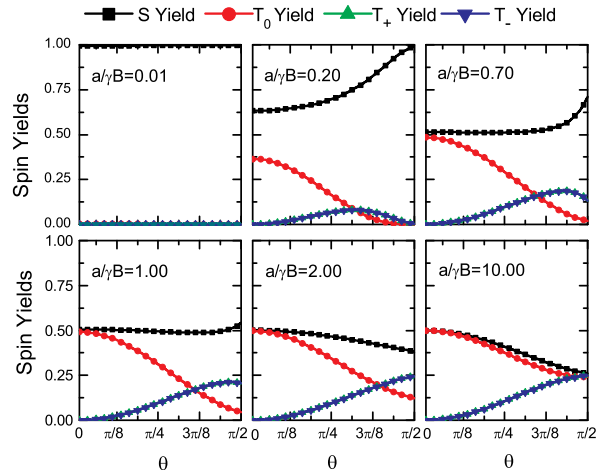


FIG. 5. (Color online) Singlet (S) and triplet (T_0, T_+, T_-) yields vs. geomagnetic field orientation for various hyperfine coupling strengths. Now the spin state of the nucleus and radical pair are disentangled. Unlike Fig. 1, the peaks in singlet yield do not appear here. This confirms that the peaks in singlet yield (Fig. 1) are direct manifestation of nuclear decoherence.

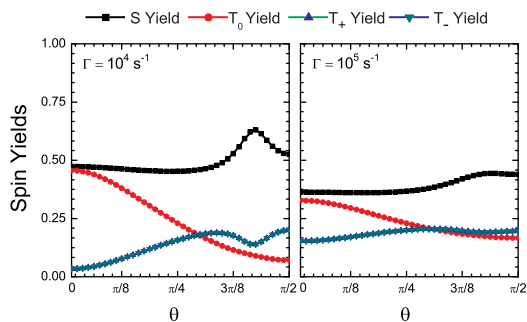


FIG. 6. (Color online) Singlet (S) and Triplet (T_0, T_+, T_-) yields vs geomagnetic field orientation in presence of environmental noise with noise rate ($\Gamma = 10^4 \text{ s}^{-1}$ and 10^5 s^{-1}). The figures shows that spin yields tend to become uniform as the environmental noise rate is increased. Thus environmental noise opens the spin transition pathways between all four spin states of the radical pair.

peaks in singlet yield have disappeared, indicating that these are due to nuclear decoherence.

Appendix C: Effect of Environmental Decoherence on All Spin Yields

The effect of environmental noise on singlet yield has been shown in Fig. 4. Fig. 6 displays the effect of environmental noise on all spin yields (S, T_0, T_+, T_-) for environmental noise rates of $10^4 s^{-1}$ and $10^5 s^{-1}$. Here we

observe that as the noise rate is increased, the yield corresponding to all spins tends to converge to 0.25. Thus, this plot establishes the fact that environmental noise opens up the spin transition pathways between the singlet state and all triplet states and thereby homogenizing the yields corresponding to all the spin states. Thus environmental noise washes away the sensitivity of the avian compass.

-
- [1] G. S. Engel, T. R. Calhoun, E. L. Read, T.-K. Ahn, T. Mančal, Y.-C. Cheng, R. E. Blankenship, and G. R. Fleming, *Nature* **446**, 782 (2007).
- [2] M. B. Plenio and S. F. Huelga, *New Journal of Physics* **10**, 113019 (2008).
- [3] N. Lambert, Y.-N. Chen, Y.-C. Cheng, C.-M. Li, G.-Y. Chen, and F. Nori, *Nature Physics* **9**, 10 (2013).
- [4] M. Mohseni, P. Rebentrost, S. Lloyd, and A. Aspuru-Guzik, *The Journal of chemical physics* **129**, 174106 (2008).
- [5] G. D. Scholes, G. R. Fleming, A. Olaya-Castro, and R. van Grondelle, *Nature chemistry* **3**, 763 (2011).
- [6] L. Turin, *Chemical Senses* **21**, 773 (1996).
- [7] J. C. Brookes, F. Hartoutsiou, A. Horsfield, and A. Stoneham, *Physical review letters* **98**, 038101 (2007).
- [8] Z. D. Nagel and J. P. Klinman, *Chemical reviews* **106**, 3095 (2006).
- [9] W. Wiltschko and R. Wiltschko, *Science* **176**, 62 (1972).
- [10] K. Schulten, C. E. Swenberg, and A. Weller, *Z. Phys. Chem* **111**, 1 (1978).
- [11] R. Wiltschko, K. Stapput, P. Thalau, and W. Wiltschko, *Journal of The Royal Society Interface* **7**, S163 (2010).
- [12] U. E. Steiner and T. Ulrich, *Chemical Reviews* **89**, 51 (1989).
- [13] T. Ritz, S. Adem, and K. Schulten, *Biophysical journal* **78**, 707 (2000).
- [14] I. A. Solov'yov and K. Schulten, *Biophysical journal* **96**, 4804 (2009).
- [15] I. A. Solov'yov and K. Schulten, *The Journal of Physical Chemistry B* **116**, 1089 (2012).
- [16] C. R. Timmel and K. B. Henbest, *Philosophical Transactions of the Royal Society of London. Series A: Mathematical, Physical and Engineering Sciences* **362**, 2573 (2004).
- [17] T. Miura, K. Maeda, and T. Arai, *The Journal of Physical Chemistry A* **110**, 4151 (2006).
- [18] C. T. Rodgers, *Pure & Applied Chemistry* **81** (2009).
- [19] J. Lau, *Spin-selective chemical reactions in radical pair magnetoreception*, Ph.D. thesis, University of Oxford (2014).
- [20] W. Wiltschko, U. Munro, H. Ford, and R. Wiltschko, (1993).
- [21] T. Ritz, R. Wiltschko, P. Hore, C. T. Rodgers, K. Stapput, P. Thalau, C. R. Timmel, and W. Wiltschko, *Biophysical journal* **96**, 3451 (2009).
- [22] M. Tiersch and H. J. Briegel, *Philosophical Transactions of the Royal Society A: Mathematical, Physical and Engineering Sciences* **370**, 4517 (2012).
- [23] T. Ritz, P. Thalau, J. B. Phillips, R. Wiltschko, and W. Wiltschko, *Nature* **429**, 177 (2004).
- [24] J. Cai, G. G. Guerreschi, and H. J. Briegel, *Physical review letters* **104**, 220502 (2010).
- [25] J. Cai and M. B. Plenio, *Physical Review Letters* **111**, 230503 (2013).
- [26] I. K. Kominis, *Physical Review E* **80**, 056115 (2009).
- [27] E. M. Gauger, E. Rieper, J. J. Morton, S. C. Benjamin, and V. Vedral, *Physical review letters* **106**, 040503 (2011).
- [28] J. N. Bandyopadhyay, T. Paterek, and D. Kaszlikowski, *Physical Review Letters* **109**, 110502 (2012).
- [29] V. S. Poonia, D. Saha, and S. Ganguly, *Workshop on Quantum Effects in Biological Systems*, Singapore, (2014).
- [30] J. Cai, F. Caruso, and M. B. Plenio, *Physical Review A* **85**, 040304 (2012).
- [31] C. Timmel, U. Till, B. Brocklehurst, K. McLauchlan, and P. Hore, *Molecular Physics* **95**, 71 (1998).
- [32] B.-M. Xu, J. Zou, H. Li, J.-G. Li, and B. Shao, *Physical Review E* **90**, 042711 (2014).
- [33] T. Baumgratz, M. Cramer, and M. B. Plenio, *Phys. Rev. Lett.* **113**, 140401 (2014).
- [34] M. W. Doherty, N. B. Manson, P. Delaney, F. Jelezko, J. Wrachtrup, and L. C. Hollenberg, *Physics Reports* **528**, 1 (2013).
- [35] J. Maze, P. Stanwix, J. Hodges, S. Hong, J. Taylor, P. Cappellaro, L. Jiang, M. G. Dutt, E. Togan, A. Zibrov, *et al.*, *Nature* **455**, 644 (2008).
- [36] G. Balasubramanian, P. Neumann, D. Twitchen, M. Markham, R. Kolesov, N. Mizuochi, J. Isoya, J. Achard, J. Beck, J. Tissler, *et al.*, *Nature materials* **8**, 383 (2009).